AIR FLUORESCENCE DETECTION OF LARGE AIR SHOWERS BELOW THE HORIZON

Peter Halverson and Theodore Bowen
Department of Physics
University of Arizona, Tucson, AZ 85721, USA

In the interest of exploring the cosmic ray spectrum at energies greater than 10^{18} eV, where flux rates at the earth's surface drop below 100 yr^{-1} km^{-2} sr^{-1}, cosmic ray physicists have been forced to construct ever larger detectors in order to collect useful amounts of data in reasonable lengths of time. At present, the ultimate example of this trend is the Fly's Eye system[1] in Utah, which uses the atmosphere around an array of skyward-looking photomultiplier tubes. The air acts as a scintillator to give detecting areas as large as 5000 km^2 sr (for highest energy events). This experiment has revealed structure (and a possible cutoff) in the ultra-high energy region above 10^{19} eV.[2]

The success of the Fly's Eye experiment provides impetus for continuing the development of larger detectors to make accessible even higher energies. However, due to the rapidly falling flux, a tenfold increase in observable energy would call for a hundredfold increase in the detecting area. But, the cost of expanding the Fly's Eye detecting area will approximately scale linearly with area.

It is for these reasons that the authors have proposed a new approach[3] to using the atmosphere as a scintillator; one which will require fewer photomultipliers, less hardware (thus being less expensive), yet will provide position and shower size information.

The Side-Looking Air Shower Detector.   As shown in Fig. 1, the Side-Looking Detector (SLD) consists of an array of at least three SLD stations, each containing six photomultipliers, a large cylindrical focusing mirror, and some associated electronics such as PMT power supplies, digitizing modules, and communication equipment (to transmit the digital data to the base station).

Each SLD station would look almost horizontally, dividing the atmosphere into a stack of three wedges 60 degrees wide and 0.2 degrees thick. The three detector stations are identical and are located at the three corners of an equilateral triangle, so their fields of view overlap. Since the detector stations are expected to be able to detect 10^{19} eV events up to 30 kilometers away, our detecting area would be about 380 km^2. If we can detect larger events up to 35 km away, then our detector area will grow to 520 km^2. A cosmic ray shower descending through the atmosphere above the detecting area successively passes through the three wedges of air, whereupon near-ultraviolet photons from excited nitrogen molecules are emitted.

As shown in Fig. 2, the photons are collected by the mirrors in the SLD stations and are focused onto long strips of acrylic that have been doped with the wavelength-shifting chemical BBQ. The BBQ absorbs the ultraviolet photons and re-emits them as green photons, which travel down the plastic strips to PMT's at each end. The PMT's convert the light from the BBQ to photoelectrons which, after being waveform digitized, are transmitted to the base station for data
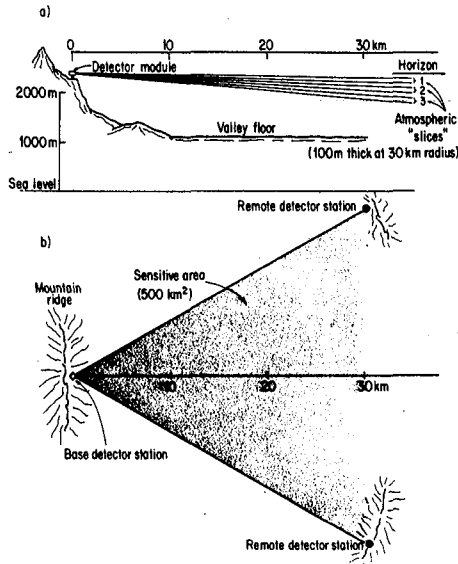
Fig. 1. Proposed side-looking air fluorescence detector to observe $E \geq 10^{19}$ eV air showers. (a) Side view (Vertical scale: X10), showing three slices or wedges (opening angles ~0.2°) viewed by each station. Viewing angles are set below the horizon to reduce background light; (b) Plan view, showing suggested triangular coverage of three stations, each having a horizontal viewing wedge angle of 60°.

analysis. The amplitude and timing information in the light pulses resulting from the passage of the cosmic ray shower contains information about the shower's location, orientation, and energy. The location and distance from the detector stations of the shower can be determined by accurately comparing the arrival times of the light pulses at each station and for each wedge. By comparing the arrival times of the photons in the upper and lower wedges at each station, the orientation of the shower may be determined. Once the distance of the shower from the SLD stations has been computed, the size of the light pulses can be used to compute the shower size. With stations located at the three corners of a triangle, the corrections required for atmospheric light attenuation can be computed from the data, as well as from calibration light flashes sent from one station to another. The calibration flashes would also synchronize the timing at the remote stations.
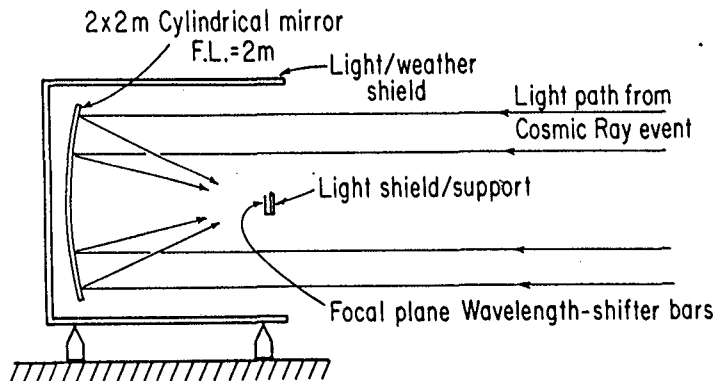

Fig. 2. Side view of proposed SLD station.

Design Equations. If S is the number of photoelectrons due to the shower, and $b\tau$ is the number of photoelectrons due to background light in time interval τ, then the fractional error is given by $\sigma(S)/S=(S+b\tau)^{1/2}/S$, which must be $\ll 1$ for a useful measurement. It is convenient to define a figure of merit M, which is the square of the reciprocal of the fractional error; $M \equiv S^2/(S+b\tau) \gg 1$ for a useful measurement. It can be shown that $M = K_1/[(1/\delta)+K_2(1+(\ell/r\delta)^2)^{1/2}]$, where $K_1 = [qN_eA\epsilon]/[4\pi r \exp(\alpha r)]$, and $K_2 = [4\pi\beta I_{sky}\Delta\lambda\phi r^2 \exp(\alpha r)]/[qN_ec]$. In these equations, q = no. of optical air fluorescence photons per meter of shower electron track (~3), N_e = no. of shower electrons, A = area of SLD mirror, ϵ = combined wavelength shifter and photocathode efficiency, α = attenuation coefficient for light transmission in air, r = distance from detector to shower, I_{sky} = no. photons/m^2-s-sr-Å in night sky (~4×10^8), β = intensity reduction factor due to viewing below horizon (~0.4), $\Delta\lambda$ = effective bandwidth of detector (~90 nm), ℓ = lateral size of shower (~100 m), c = speed of light, ϕ = horizontal opening angle of viewing wedge (1.047 rad), and δ = its vertical opening angle. As δ increases, M approaches a maximum possible value, K_1/K_2, because the time interval τ increases with δ. If $A\epsilon$ is chosen to be 0.25 m^2 and N_e is 8×10^9 electrons for an event at r = 30 km, then K_1/K_2 = 9.3 and M = 4.9 if δ = 0.2° (τ~0.5 µs).

The Scintillation Efficiency of Air. We have carried out a small experiment using ground-level muons in the laboratory to confirm that the yield of photons per meter, q, into a PMT with bialkali response is 3.2±0.5 photons/meter. A black box was employed so Cherenkov photons would be absorbed; most ground-level muons are near or below the Cherenkov threshold in air, so the black walls appear to reduce the Cherenkov component to a negligible level relative to air fluorescence. The yield was obtained from the counting efficiency for single-photoelectron pulses in a 5 inch RCA 4522 PMT viewing 20.3 cm of path.
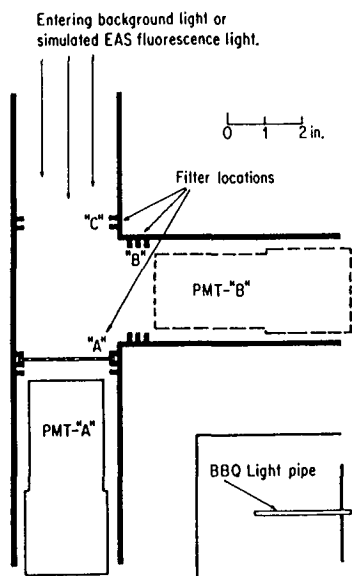

Fig. 3.

The Effect of Filters on Signal and Background. The apparatus used in making these measurements is shown in Fig. 3. The transmission coefficient of each filter was measured by comparing the output current of an RCA 6655A photomultiplier having S11 response with and without the filter in place. Two sets of data were gathered: filter performance on background light, as observed from Mount Hopkins, and filter performance on light from each of the major air fluorescence lines, as produced by a monochrometer. Table I shows the factor by which the figure-of-merit, M, is predicted to improve with the use of each filter. The emission spectrum predicted by Bunner[4] was employed in the calculations. The distance between the air shower and the detector must be specified because the attenuation due to Rayleigh scattering significantly modifies the source spectrum.

Since the signal-to-background ratio tends to be smallest for the most distant events, the UG-5 and U330 filters have the most favorable characteristics among those listed. Filtering also attenuates the signals; this must be considered along with the improvement factors. If a filter with ≥70% transmission for the 3914 and 4000 Å bands could be found, it would be better than any of those listed in Table I.

Table I. Expected figure-of-merit improvement factors for various filters.

Event Distance [km]	Filter:	UG-1	UG-5	U330	U340
0		5.0	4.8	4.6	4.1
4		4.4	4.5	4.2	3.3
16		2.7	3.5	3.3	1.4
32		1.6	2.8	2.7	0.5

The Effect of Viewing Below the Horizon. The background light intensity I_T, below the horizon at Mount Hopkins, Arizona was compared with the dark night sky intensity I_0. At each angle, the distance to the valley floor could be calculated. Figure 4 shows I_T/I_0 as a function of the g/cm^2 of air between the detector and the valley floor. As shown by the curves, the data seem to agree with a model in which the below-horizon background is due to Rayleigh-scattered light; for this model I_T/I_0 approaches 0.5 for infinite air thickness.
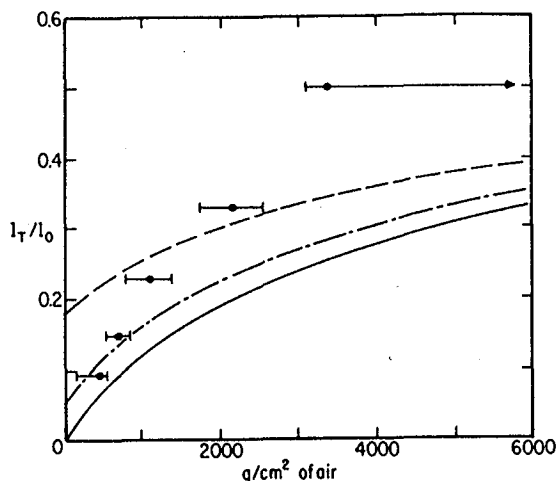

Fig. 4, Plot of scattered light observed at Mt. Hopkins as a function of air thickness to the ground. The theoretical curves are for 0%, 5%, and 18% (solid, dot-dashed, and dashed, respectively) ground reflectivities.

Conclusion. Filters and below-horizon viewing may offer important advantages for an economical side-looking air fluorescence detector.

1. R. Cady et al., "The Fly's Eye," Report UUHEP-83/11, University of Utah, 1983.

2. R. M. Baltrusaitis et al., Phys. Rev. Lett. 54 (1985).

3. T. Bowen and P. Halverson, Proceedings of Workshop on Cosmic Ray and High Energy Gamma Ray Experiments for the Space Station Era, Baton Rouge, LA, 17-20 October 1984.

4. A. N. Bunner, "Cosmic Ray Detection by Atmospheric Fluorescence," Thesis, Cornell University, 1966.